
Metabolic and Hemodynamic Evaluation of Gliomas Using Positron Emission Tomography

J.L. Tyler, M. Diksic, J-G. Villemure, A.C. Evans, E. Meyer, Y.L. Yamamoto, and W. Feindel

Brain Imaging Center, Montreal Neurological Institute and Hospital, and Department of Neurology and Neurosurgery, McGill University, Montreal, Canada

Positron emission tomography (PET) was used on 16 patients with untreated cerebral gliomas to measure cerebral glucose and oxygen metabolism, oxygen extraction, blood flow, and blood volume. In addition, pH values were obtained for seven cases. Gliomas were later proven by biopsy; two patients had tumors with degrees of malignancy of grade II, two patients had grade III, and 12 patients had grade IV tumors. Compared with homologous gray matter regions in the opposite hemisphere, tumor tissue showed increased blood volume, but decreased oxygen extraction and oxygen metabolism. Compared with grade II tumors, grade IV tumors demonstrated higher blood volumes, but lower relative oxygen extraction and utilization. Tumor blood flow was variable, but was lower in the higher grade tumors. Rates of glucose utilization in tumor, calculated by using individually determined rate constants, were variable, and did not correlate with tumor size or tumor grade. Parietal tumors ($n = 6$) tended to have higher relative glucose utilization and blood flow, and lower relative oxygen extraction, when compared with frontal tumors ($n = 4$). Tumor pH differed significantly from the pH in contralateral brain ($p < 0.005$); alkalotic pH values were consistently seen. These findings in and around cerebral gliomas studied before intervention differ from the results found in gliomas after exposure to radiation or chemotherapy.

J Nucl Med 28:1123-1133, 1987

Cerebral gliomas make up ~50% of all intracranial tumors. Despite recent advancements in microsurgical techniques, refinements in radiotherapy, and new approaches to chemotherapy, survival times remain short for high grade tumors (1). To understand the malignant process better, more must be known about the basic metabolic and hemodynamic parameters of tumors and how these influence tumor growth. This could then lead to the design of improved therapy. Positron emission tomography (PET) provides the techniques for noninvasive study of specific aspects of metabolism and perfusion in normal and malignant tissue.

Study of these neoplasms is complicated by the inherent heterogeneity of the tumors themselves, especially those of higher grade. Data from previous studies (2-4) have been based on nonhomogeneous patient populations, including patients with newly diagnosed tumors and recurrent lesions, as well as patients with

and without surgery, radiation therapy, and/or chemotherapy. The results reported from these studies, thus, cannot be assumed to be applicable to newly diagnosed, untreated neoplasms.

For these reasons, a project was undertaken to study untreated cerebral gliomas using PET, by measuring blood flow (CBF) and volume (CBV), glucose (LCMRGI) and oxygen utilization (CMRO₂), oxygen extraction (OER), and pH.

MATERIALS AND METHODS

Patients

Sixteen subjects consisting of 11 males and five nonpregnant females were entered into the research protocol. All were referred to our institution for evaluation of an intracerebral space-occupying lesion suspected of being a high grade glioma. All patients had a Karnofsky neurologic performance status (5) of 50% or greater, and were able to give informed consent. All patients were studied with PET before any intervention; none had prior surgery, chemotherapy, or radiation therapy. Following metabolic and hemodynamic evaluation with PET, the pathology of the intracerebral lesion was determined by biopsy.

Received July 24, 1986; revision accepted Feb. 4, 1987.

For reprints contact: Jane L. Tyler, MD, Brain Imaging Center, Montreal Neurological Institute, 3801 University St., Montreal, Quebec, H3A 2B4 Canada.

Positron Emission Tomography

Positron emission tomography scans were collected on the Therascan 3128 positron tomograph (6), a two-ring scanner containing 64 bismuth germanate (BGO) detectors per ring. Both direct and cross-slice coincidences were acquired, with three slices obtained simultaneously. Image resolution was 12 mm (full width at half maximum) in both the transaxial and axial directions. Images were reconstructed using the Therascan software package (6–9).

Cerebral glucose metabolism. Fluorine-18- (^{18}F) labeled fluorodeoxyglucose (FDG) was prepared on site (10); the specific activity was 680 mCi/mmol. Patients received a 5-mCi bolus of [^{18}F]FDG injected intravenously over 1 min. Beginning simultaneously with the initiation of the FDG injection, rapid sequential scans were obtained in order to measure the FDG kinetic rate constants and to monitor the uptake and fixation of the isotope in cerebral tissue (11). Blood samples for determination of ^{18}F plasma activity and glucose concentration were taken from the opposite arm, using direct arterial sampling. Forty minutes after the injection of the [^{18}F]FDG, three medium resolution tomographic slices were obtained simultaneously at each of two scan positions, encompassing the tumor site as well as distant cerebral tissue. Two to 5 million true coincidences were obtained per slice in these static scans.

The analysis of the static FDG scans was based on Phelps et al.'s (12) adaptation of the Sokoloff method (13); in addition, a reformulation of the operational equation suggested by Brooks was incorporated (14). The value of the lumped constant used was that established by Huang (15). Fluorodeoxyglucose rate constants k_1 , k_2 , and k_3 were calculated for each region studied using data obtained during the dynamic FDG study (11). In the latter procedure, the errors in rate constant determination caused by vascular activity were reduced by explicit inclusion of the regional blood volume (rCBV) as a fit parameter.

Cerebral blood flow, blood volume, oxygen extraction, oxygen metabolism. Oxygen-15- (^{15}O) labeled gases, O_2 , CO_2 , and CO , were administered sequentially in one session to provide three separate datasets. These were combined to provide functional maps for blood flow (CBF), oxygen extraction fraction (OER), oxygen metabolic rate (rCMRO₂), and blood volume (CBV) using the methodology of Frackowiak et al. (16).

The $^{15}\text{O}-\text{O}_2$ and $^{15}\text{O}-\text{CO}_2$ gases were delivered continuously during the study period at flows of 10 mCi/min at 80 cc/min, and 5 mCi/min at 60 cc/min, respectively. Labeled gases were mixed with 200 cc/min of medical air, and were supplied to the patient through a plastic face mask. Once inhalation of the labeled gas was initiated, equilibrium was established over a 12-min period, followed by medium resolution scans (transverse resolution = 12 mm FWHM) at the positions described for the ^{18}F FDG study. Typically, 1.5–2.5 million true events were recorded for each $^{15}\text{O}-\text{O}_2$ image, and 2–4 million for each $^{15}\text{O}-\text{CO}_2$ image.

$^{15}\text{O}-\text{CO}$ was administered at a dose rate of 80 mCi/min at 100 cc/min for 4 min. The $^{15}\text{O}-\text{CO}$ supply was then discontinued, and after a 1-min equilibration period, low resolution images (transverse resolution = 19.5 mm FWHM) were obtained at the two scan positions. Three hundred to five hundred thousand typical images contained true coincidences. Throughout these studies, blood samples were obtained (with-

drawn over 15–20 sec) from an arterial line for the measurement of blood and plasma radioactivity as well as determination of blood gases.

The oxygen analysis program generated maps for the four functional parameters (CBF, CBV, OER, and CMRO₂) for each anatomic plane as a composite dataset. OER and CMRO₂ images were corrected for CBV (17).

Cerebral pH. The cerebral pH was determined using carbon-11 (^{11}C)-5,5-dimethyl-2,4-oxazolidinedione (DMO) according to the method of Kearfott et al. (18) and Rottenberg et al. (19). [^{11}C]DMO was injected as a 30-mCi bolus, and low resolution dynamic scans were obtained over 30 min. Subsequently, the patient was scanned in the "high" resolution mode in two positions through the tumor mass. Blood samples were taken throughout the scanning time to obtain values for plasma pH and carbon-11 (^{11}C) radioactivity. Cerebral pH maps were produced according to the equation:

$$\text{rCpH} = \log_{10} R(10^{\text{pHb}} + 10^{\text{pKa}}) - 10^{\text{pKa}}, \quad (1)$$

where rCpH is cerebral pH, pHb is plasma pH, pKa is the pK for DMO, and R represents the ratio of tissue to plasma radioactivity. All pH measurements were corrected for CBV.

Image analysis. All studies were examined by placing circular regions of interest (ROI) 9 mm in diameter over cortical gray matter areas and over the main bulk of tumor tissue. The location and extent of the tumors were judged by comparing the functional PET images with computed tomography (CT) scans and/or magnetic resonance imaging (MRI) scans obtained at the same levels. As the size of the tumor allowed, multiple ROI over several PET scan levels were examined and averaged to obtain a mean functional value. In cases where there was a cystic portion of the tumor, regions were chosen along the tumor rim. For the analysis of the FDG images, in addition to mean values for multiple ROI in the main tumor bulk, the range of LCMRGI values through the tumor was determined by examining multiple profiles through the tumor. The highest and lowest pixel values were then determined, in order for this data to be compared with previous studies using different FDG analysis techniques (2). For the analysis of DMO images, ROI examined in the hemisphere contralateral to the tumor were placed in locations that were exact mirror images of the ROI placed over the tumor; in certain instances this resulted in contralateral ROI encompassing white matter, and occasionally ventricle, along with gray matter.

Values for the tumor hemodynamic and metabolic parameters were compared using a least squares fit. In particular, possible correlations between CBF and LCMRGI and CMRO₂, and between MR and CBV and pH were examined.

RESULTS

Sixteen patients suspected of having intracerebral gliomas on the basis of history, physical exam, and CT scan were entered into the protocol. Eleven subjects were male and five were female, the average age was 51 years (range 23–78 yr). The tumor locations and CT scan findings are presented in Table 1.

All patients had PET measurements of LCMRGI, CBF, CBV, OER, and CMRO₂. Due to technical diffi-

TABLE 1
Patient Population with Intracerebral Gliomas

Patient no.	Age/sex	Tumor location	Histologic Grade	CT enhancement
1	72/F	R-midfrontal	IV	+
2	37/M	L-thalamus	III	Weak +
3	76/F	L-thalamus	IV	+
4	59/M	R-parietal	II	+
5	50/F	R-parieto-occipital	IV	+
6	78/M	L-temporal	IV	Infusion not done
7	40/M	L-frontal	II	—
8	70/M	R-parietal	IV	+
9	23/F	L-frontoparietal	IV	+
10	25/M	L-frontal	III	+
11	58/M	L-frontal	IV	+
12	35/M	thalamus	IV	Weak +
13	49/F	L-centrum ovale	IV	+
14	58/M	R-parietal	IV	+
15	29/M	R-parietal	IV	+
16	55/M	L-parietal/periventricular	IV	+

culties, pH measurements were obtained in only seven patients, and dynamic FDG studies with measurement of individual rate constants were not performed in four of the 15 (Patients 3, 6, 8, and 11). The rate constants of Huang (15) were used in the calculation of LCMRGI

values in these four cases. The findings are presented in Table 2; patient data were assessed in relation to normal control values at this institution.*

Overall, tumor CBF was variable, and tended to be lower, and more varied, in the higher grade lesions (mean = 31 ± 16 cc/100 g/min versus 43 cc/100 g/min). Tumor CBV was increased by an average of 1.8 times the values in healthy controls, with values higher and more varied in the grade III and IV neoplasms relative to grade II tumors ($5.8 \pm 1.8\%$ versus $4.8 \pm 0.6\%$). Tumor OER was within the normal range in six cases (38%) and decreased by an average of 50% below normal in the remainder. CMRO₂ was decreased in all tumors, and was significantly lower in the high grade cases compared with the two grade II tumors (mean = 72 ± 24 μmol/100 g/min versus 122 μmol/100 g/min). LCMRGI values were low in the tumors, averaging 40% lower than normal control values, however, LCMRGI values did not differ significantly between low and high grade gliomas.

Metabolic and hemodynamic findings in tumor and in a homologous gray matter region in contralateral hemisphere were compared; the results for the 16 patients with gliomas are listed in Table 3. CBF ratios of tumor to contralateral brain were more variable in the

TABLE 2
Metabolic and Hemodynamic Results in 16 Patients with Gliomas

Patient no.	Tumor grade	LCMRGI [†]		CBF [†]	CBV [‡]	OER [§]	CMRO ₂	MR [¶] = CMRO ₂ /LCMRGI	pH
		Mean	Range						
4	II	22	(17-31)	43	4.3	0.41	132	6.00	—
7	II	25	(20-34)	46	5.9	0.29	112	4.48	—
Mean		23.5		45	4.8	0.35	122	5.24	
±s.d.		±2.1		±2	±0.6	±0.08	±14	±1.07	
10	III	25	(10-38)	14	3.6	0.46	66	2.64	7.34
2	III	28	(12-31)	63	5.4	0.15	106	3.79	—
1	IV	19	(8-35)	31	7.3	0.27	80	4.21	—
3	IV	35*	(32-37)	45	5.1	0.18	69	1.97	—
5	IV	32	(25-53)	62	8.2	0.13	102	3.19	7.35
6	IV	39*	(20-65)	30	6.0	0.25	62	1.59	—
8	IV	24*	(15-35)	24	3.8	0.21	42	1.75	—
9	IV	42	(24-56)	25	10.0	0.12	25	0.60	—
11	IV	25*	(20-39)	20	4.2	0.40	77	3.08	—
12	IV	27	(19-42)	42	5.7	0.21	90	3.33	6.99
13	IV	25	(19-33)	23	6.4	0.42	88	3.52	6.81
14	IV	16	(10-22)	13	3.7	0.44	65	4.06	7.06
15	IV	18	(10-25)	19	6.3	0.27	46	2.56	7.43
16	IV	23	(18-26)	20	5.9	0.40	109	4.74	7.18
Mean		27		31	5.8	0.28	73	2.93	
±s.d.		±7.7		±16	±1.8	±0.12	±25	±1.15	

* LCMRGI (local cerebral metabolic rate for glucose) in μmol/100 g tissue/min [* calculated using the rate constants of Huang et al. (12), others calculated with individually derived rate constants (10)].

† CBF (cerebral blood flow) in cc/100 g/min.

‡ CBV (cerebral blood volume) as a fraction of 100%.

§ OER (oxygen extraction fraction) as a percentage of 1.00.

|| CMRO₂ (cerebral metabolic rate for oxygen) in μmol/100 g tissue/min.

¶ MR (metabolic rate) as the ratio of oxygen to glucose utilization.

TABLE 3
Metabolic Ratios: Tumor to Contralateral Brain

Patient no.	Tumor grade	LCMRGI	CBF	OER	CBV	CMRO ₂
4	II	0.91	0.95	1.02	0.97	0.83
7	II	1.09	0.83	1.00	1.40	0.83
Mean		1.00	0.89	1.01	1.19	0.83
±s.d.		±0.13	±0.09	±0.01	±0.30	0
10	III	0.64	0.56	0.84	1.12	0.52
2	III	1.33	1.20	0.33	1.08	0.62
1	IV	0.58	0.40	0.62	2.23	0.67
3	IV	1.25 [*]	1.10	0.47	1.02	0.36
5	IV	1.53	2.09	0.21	2.38	0.40
6	IV	0.81 [*]	0.53	0.67	1.59	0.53
8	IV	0.69 [*]	0.65	0.48	1.36	0.30
9	IV	1.89	1.45	0.34	1.07	0.27
11	IV	0.86 [*]	0.77	0.66	1.14	0.55
12	IV	0.89	1.22	0.42	1.04	0.58
13	IV	1.01	0.48	0.46	1.31	0.52
14	IV	0.59	0.56	0.59	1.13	0.65
15	IV	0.56	0.70	0.51	1.17	0.35
16	IV	0.82	0.87	0.57	1.48	0.78
Mean		0.96	0.90	0.51	1.37	0.51
±s.d.		±0.40	±0.47	±0.16	±0.43	±0.15

^{*}LCMRGI calculated with Huang's rate constants. All other LCMRGI values calculated using individually determined rate constants.

high grade tumors, but overall the ratios did not differ between low and high grade gliomas. Ratios of OER and CMRO₂ were much lower, but CBV ratios were considerably higher in the grade III and IV tumors. LCMRGI ratios were variable, but tended to be slightly lower in the high grade tumors. Greater variability was seen in the LCMRGI ratios (range, 0.56–1.89) than in the CMRO₂ ratios (range, 0.27–0.78).

The metabolic ratio, or the ratio of oxygen to glucose utilization, averaged 2.9 ± 1.2 (range, 0.6–4.2) in the grade III and IV tumors. Fifty-seven percent of the grade III or IV tumors had metabolic ratio values within 2 standard deviations (s.d.) of published normal control values (5.2 ± 1.2) (20). The two cases of grade II tumors had metabolic ratios of 6.00 and 4.48.

TABLE 4
High Grade Tumor pH, and Metabolic Ratio (MR)

Patient	Tumor grade	Tumor pH	Contralateral brain pH	Tumor MR
15	IV	7.43	7.09	2.56
5	IV	7.35	7.14	3.19
10	III	7.34	7.10	2.64
16	IV	7.18	7.16	4.74
14	IV	7.06	6.84	4.06
12	IV	6.99	6.83	3.33
13	IV	6.81	6.73	3.52

TABLE 5
Tumor to Contralateral Brain Metabolic Ratios by Tumor Location

	Frontal (n = 5)	Parietal (n = 6)	Thalamic (n = 3)
LCMRGI	0.94 ± 0.55	1.09 ± 0.55	1.22 ± 0.32
CBF	0.80 ± 0.40	1.07 ± 0.60	1.17 ± 0.06
OER	0.69 ± 0.25	0.53 ± 0.28	0.41 ± 0.07
CBV	1.39 ± 0.49	1.35 ± 0.52	1.05 ± 0.03
CMRO ₂	0.57 ± 0.21	0.48 ± 0.22	0.52 ± 0.14
MR	0.42 ± 0.24	0.59 ± 0.37	0.34 ± 0.09

Tumor pH (Table 4) was consistently higher than the pH in the ROI in the contralateral hemisphere. In this small series, no correlation could be found between tumor and contralateral brain pH, and tumor metabolic ratio.

The metabolic and hemodynamic parameters were examined on the basis of tumor location (Table 5). In these small groups, no significant difference was seen in the CMRO₂ ratios between tumor and contralateral gray matter when the tumor site was considered. However, the thalamic tumors (n = 3) were seen to have lower ratios for OER, CMRO₂, and CBV, and higher ratios for CBF and LCMRGI compared with the frontal (n = 5) and parietal (n = 6) lesions, although when a t-test comparison was used, these findings were not significant at the $p < 0.10$ level.

When linear regression was used to compare the results of various metabolic and hemodynamic parameters in tumor tissue, no correlation was found between LCMRGI and CBF ($y = 0.15x + 21.75$; $r = 0.325$), between CMRO₂ and CBF ($y = 1.00x + 47.08$; $r = 0.550$), or between metabolic ratio and pH ($y = 1.57x + 14.65$; $r = 0.456$).

The tumors were often seen to have metabolic effects remote from the actual tumor location. Eleven of the 16 patients had global (whole brain) decreases in LCMRGI, six of which had a greater decrease in the hemisphere containing the tumor. An additional four patients had decreased LCMRGI in the entire hemisphere containing the tumor, with normal range values in the contralateral hemisphere. Only one patient (Patient 10) with a frontal tumor had no evidence of LCMRGI depression distant from the tumor. The average hemispheric depression of LCMRGI seen was ~35%. Six patients had global decreases in CMRO₂, two with predominance in the hemisphere containing the tumor. Two other patients had diffusely decreased CMRO₂ only in the hemisphere containing the tumor. The decreases in CMRO₂ were accompanied by smaller decreases in CBF, without a concomitant rise in OER.

Positron emission tomography images from two representative cases (15 and 5) are presented in Figures 1 and 2. Both cases demonstrate high CBV, low OER, and low CMRO₂ in tumor tissue. However, Patient 15

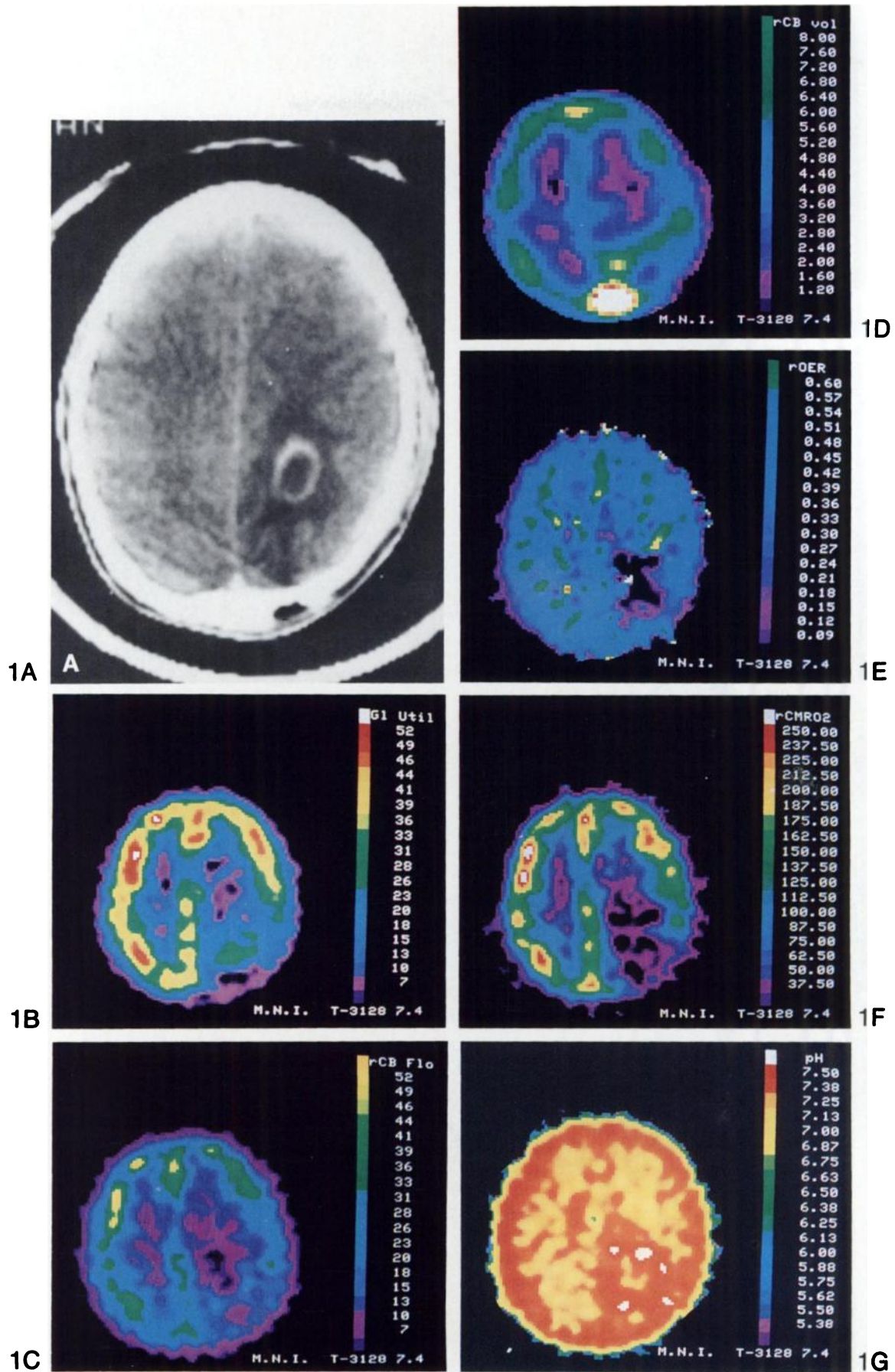


FIGURE 1 Grade IV glioma of the right parietal region in a 29-yr-old male the tumor seen on CT scan (A), was seen low LCMRGI (B), low CBF (C), high CBV (D), low OER (E) and CMRO₂ (F) and alkalotic pH (G). All CT and PET images are oriented with the right cerebral hemisphere to the right in the picture.

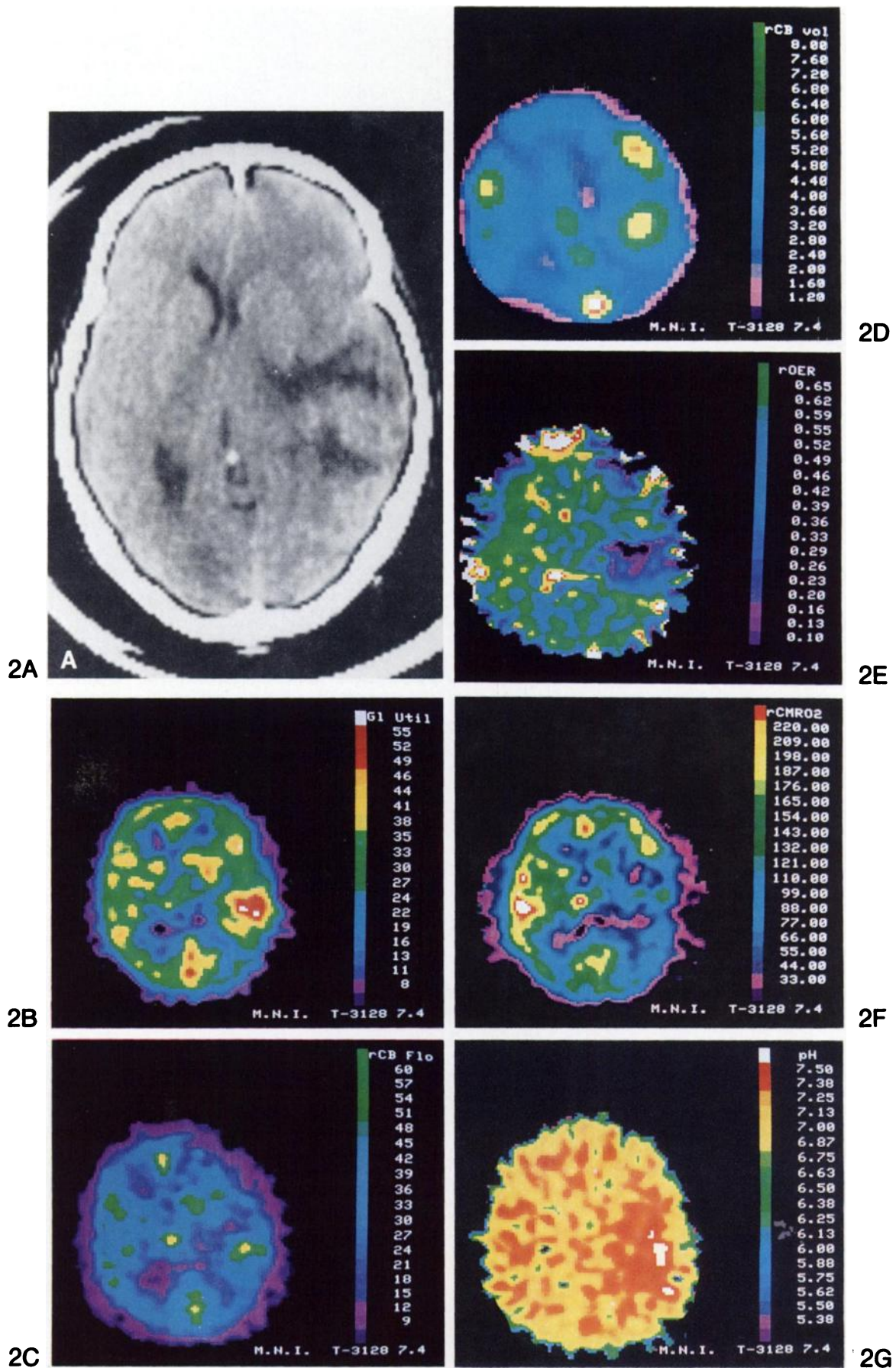


FIGURE 2

Grade IV glioma of the right parieto-occipital region in a 50-yr-old female (A), demonstrating normal range glucose metabolism, which represented a relatively high LCMRGI compared to the rest of the cortex (B). This tumor demonstrated high CBF (C), high CBV (D), low OER (E) and CMRO₂ (F) and alkalotic pH (G). All CT and PET images are oriented with the right cerebral hemisphere to the right in the picture.

demonstrated low LCMRGI and low CBF in the tumor, whereas, Patient 5 demonstrated high values of both LCMRGI and CBF in tumor. The CBV image is slightly larger than the corresponding flow and metabolism images for two reasons. Principally, the CBV image includes activity located in extracerebral vessels and consequently will appear to represent a larger brain. Secondly, the CBV image is derived using ^{15}O and low-resolution reconstruction (transverse resolution = 19 mm FWHM), which will tend to blur the image at the edges. CBV images collected at higher resolution (12 mm FWHM) with the longer-lived ^{11}C label are only marginally smaller, confirming that the major cause of the apparent size disparity is physiologic, rather than methodologic, in nature.

DISCUSSION

Positron emission tomography provides a unique opportunity to study physiologic processes in a noninvasive manner. This capability has been applied here to the study of cerebral gliomas, using PET to evaluate metabolic and hemodynamic parameters in these lesions. Current acceptable therapy for gliomas involves drugs and/or radiation aimed at disrupting the pathologic growth of these tumors, with as little deleterious effect as possible on surrounding brain. To this end, it is crucial to understand the physiology of human gliomas in vivo, and how that differs from the physiology of normal brain.

The present work was undertaken to study cerebral blood flow and volume, oxygen extraction, oxygen and glucose utilization, and pH in a group of patients with cerebral gliomas before they had undergone surgery, chemotherapy, or radiation treatment. Previous PET studies of malignant gliomas generally have failed to measure multiple parameters in the same patient, and several studies have included patients after radiation therapy and/or chemotherapy (2-4). Because it is known that chemotherapy and radiotherapy, themselves, cause changes in tumor as well as surrounding brain (21-23) and because primary and recurrent glioblastomas differ in their metabolism (24), we elected to study only patients before initiation of any therapy.

The present study demonstrated variable CBF, high CBV, and low CMRO_2 in untreated gliomas (Table 2). The variable flow reported is similar to findings in animal studies (25-30). Low CMRO_2 values are in keeping with the relatively anaerobic energy metabolism in tumors and, as in previous work (31) CMRO_2 in this study was decreased to a greater extent than was CBF. The low OER implies that the tumor is not ischemic however, and that perfusion is sufficient to meet the metabolic need for oxygen. This finding is not in keeping with a body of experimental work supporting the theory that a proportion of tumor cells are relatively

deprived of oxygen (32). This apparent discrepancy may be due in part to the relatively large resolution volumes for PET scanners. Due to relatively poor spatial resolution of PET scanning, the presence of small ischemic foci may not be detected, and a thin rim of tumor around a cystic/necrotic center may not be adequately resolved. Also, quantitative artifacts may be introduced by the ^{15}O model, itself. Measurements of CBF with ^{15}O - CO_2 may be inaccurate in pathologic situations, in which the brain-blood partition coefficient cannot be assumed to be uniform over the entire brain slice (33). Inaccuracies in the ^{15}O - CO_2 study, at the same time would affect the OER and CMRO_2 computations (16). Arteriovenous shunting, resulting in an effective increase in arterial blood volume, would increase the background activity during the ^{15}O - O_2 study, due to nonextracted hemoglobin-bound oxygen. However, this would not result in alterations of OER or CMRO_2 , because these parameters are corrected for CBV by the ^{15}O - CO study (15,34).

In contrast with previously published work (35), tumor CBV was found to be increased in all cases, both in the absolute value for CBV and relative to the values obtained in the contralateral cortex. This increase in tumor CBV seen here is consistent with the angiographic appearance of an increased blood-pool in malignant astrocytomas. Markedly increased vascularity is seen in one-third of cases, slight to moderately increased in one-third, and a diffuse homogeneous or ring-like blush in another 10% of cases. The remainder, roughly only 23%, appear relatively avascular on angiography (36).

The results from this present study are similar to the findings in a recent study of eight patients with brain tumors, which reported decreased blood flow, decreased oxygen extraction, and decreased oxygen utilization in the solid sections of untreated tumors (37). Included in this group, however, were a mixture of tumors: four gliomas, two metastatic carcinomas, and a malignant lymphoma; one patient did not have a biopsy. Later work by the same group examined 15 patients with untreated gliomas and found CBF very variable (32 ± 27 ml/100 g/min) and OER and CMRO_2 decreased relative to contralateral gray matter (36). In contrast to this present work, however, that study reported a decrease in tumor CBV (mean $4.3 \pm 2.1\%$) relative to control values in that lab (mean $5.9 \pm 0.6\%$).

The finding of variable and often very low LCMRGI values in the tumors is in contrast with reports by other groups studying large numbers of central nervous system neoplasms using PET (2,38), and in contrast with experimental work relating degree of malignancy to tumor metabolism (39-41). Some have suggested that hypermetabolism on FDG PET scans correlates strongly with both tumor grade (2) and survival (4), whereas, other investigators found no clear correlation

between tumor grade and LCMRGI (33). These studies, however, combined results from new tumors and recurrent lesions, and included patients who had had surgery with partial tumor resection, radiation therapy, and in some cases chemotherapy. It is clear from this present work on newly diagnosed tumors, however, that the measurements from FDG studies of tumors by PET provides information that is much more complex and variable. Given the heterogeneity of high grade gliomas, with mixtures of necrotic tissue and actively growing cells, it is not surprising that a range of glucose metabolic rates can be found within the solid part of the same tumor (Table 2). Despite this fairly large range of LCMRGI values, however, the average rate of glioma glucose metabolism was lower than that of the contralateral gray matter. The low LCMRGI values found cannot be attributed merely to an insufficient delivery of FDG to the tumor site for potential uptake. Although tumor blood flow was low in certain cases, as previously stated, no increase in OER was seen to indicate that perfusion was inadequate to meet metabolic needs. Other investigators (33) have found the tumor glucose extraction ratio to be similar to that in remote brain.

In previous studies of tumor and normal brain glucose metabolism (42), the peak value of LCMRGI in tumor was reported, and generally high LCMRGI values were seen. Once again, however, this finding was seen in a fairly heterogeneous group of tumors. In the present study, LCMRGI values from multiple ROI over the tumor were averaged; in addition, both maximum and minimum LCMRGI values were obtained. By averaging nonhomogenous substructures, the latter method cannot distinguish different metabolic states within the tumor as well. On the other hand, it is not as susceptible to the influence of surrounding structures as is the peak selection approach. In PET imaging the influence of neighboring features can have a significant impact on the apparent activity within a small region (43). Both the average and maximum LCMRGI values in this study were lower than the LCMRGI values reported from a combination of cases of both newly diagnosed and recurrent tumors.

The reason for this difference in LCMRGI between untreated and recurrent gliomas is not clear. Attempts at tumor killing with radiation or drugs may select out the most malignant cell types, which, when they multiply and are recognizable as tumor recurrence, have much more aggressive metabolic characteristics and higher rates of glucose utilization as measured by the PET-FDG technique. Alternatively, basic differences may exist in the metabolism of tumor cells before and after exposure to radiation and chemotherapy, despite a similar pathologic appearance. It is known that malignant transformation of glial cells is capable of quantitatively altering the transport of substances, including glucose, into tumor cells (44-46), and there is increased

activity of the enzymes leading to the pentose phosphate shunt in tumors (47,48). In light of alterations of normal biochemistry in tumors, the FDG model may not accurately reflect the path of glucose utilization or the total energy metabolism (e.g., utilization of glycogen or fatty acids) in these lesions.

The depression of metabolism distant from the tumor seen here also has been reported earlier (43,49). This depression could not be explained by the physical influence of an expanding tumor alone. In this remote tissue, metabolic suppression was not always accompanied by evidence of a midline shift of structures or significant edema. Neither can the metabolic suppression be fully attributed to decreased perfusion. Although peritumoral blood flow has been shown to be reduced with advanced degrees of peritumoral edema (50), a study of excised edematous human peritumoral tissue demonstrated only an 8% mean increase in gray matter volume (51). In addition, no increase in oxygen extraction (suggesting inadequate perfusion) was seen in these remote regions, and the degree of LCMRGI and CMRO₂ suppression was much greater than the decreases seen in CBF. Thus, in light of the absence of physical factors to explain this remote suppression, we agree that transneuronal interactions may be important mechanisms for this suppression (48).

The metabolic ratios (CMRO₂/LCMRGI) were within normal limits (20) in the two patients with grade II lesions. In the higher grade tumors, 21% were within 1 s.d. of normal (20), and 57% were within 2 s.d. Although in most cases this calculation represents severe decreases in both oxygen and glucose metabolism, the relationship between CMRO₂ and LCMRGI shown here does not appear as uncoupled or deranged, as predicted from previous studies (32) reporting anaerobic glycolysis in tumors.

Positron emission tomography-DMO measurements of tissue pH in this study consistently found higher values in the tumor mass than in contralateral gray matter. This is in agreement with clinical and experimental studies reported elsewhere (19,52,53), in which tumor tissue was found to be more alkaline than remote brain tissue. This finding may be due to the abnormal blood-brain barrier seen in malignant gliomas (54), with leakage of DMO into tissues, resulting in a spuriously high pH reading. This also may be partially due to the effects of an increased extracellular fluid volume in tumor tissue; measurements of extracellular fluid volume (V_e) in rats has shown higher values for V_e and higher tissue pH values in implanted RG-2 glioma tissue than in remote rat brain (52). However, in the same study (52), autoradiographic measurements of intracellular pH showed no significant difference between the tumor cells and normal brain cells, despite the presumed high rate of anaerobic glycolysis and presumed lactic acid production in tumor tissue (38).

An alternative explanation for higher glucose utilization could be found in increased activity of the pentose phosphate shunt, which would result in the production of nucleic acids, rather than the accumulation of lactate.

It is interesting to note that in this series of patients there was some tendency for tumor tissue with higher pH values to have lower metabolic ratios (Table 4). Tumors with the greatest abnormalities in metabolism may have the most severe depression of oxygen utilization, and higher shunting of glucose substrate into the pentose phosphate shunt, with less lactate production. Alternatively, pathologic changes in tissue pH, perhaps due to increased V_e , could adversely affect neuronal metabolism, or intrinsic abnormalities in tumor cell metabolism could lead to increased V_e , subsequently producing a more plasma-like pH value in tumor tissue. Full understanding of the interplay of these parameters may allow the manipulation of pH in the future in the hope of affecting the delivery and distribution of chemotherapeutic drugs or by affecting the sensitivity of tumor cells to radiation therapy through changes in regional pH.

Although the number of patients in each group was small, it was interesting to note trends in metabolic parameters based on tumor location (Table 5). It has been previously reported that glucose utilization can be an important prognostic factor for patients with recurrent frontal, parietal, and thalamic neoplasms (4). The data from this present study would suggest the possibility of inherent metabolic differences in the ratio of untreated tumor to contralateral brain for LCMRGI, CBF, CBV, OER, and metabolic ratios, based on tumor location. Clearly, larger numbers of patients must be studied to confirm these trends.

In summary, although high grade gliomas represent a fairly heterogeneous group of tumors, certain metabolic and hemodynamic similarities were seen in the present study. Decreased OER and $CMRO_2$, and increased CBV and pH appeared to be common characteristics, whereas CBF was quite variable within these tumors. LCMRGI was variable within tumors, but averaged 40% lower than control values. This finding suggests intrinsic metabolic differences between untreated tumors and tumors recurring after therapy, in which high LCMRGI values have been observed (2,4,42).

NOTE

* Normal range values obtained in nine healthy control subjects (six male, three female), mean age, 47 yr; LCMRGI = 45.4 ± 2.9 mol/100 g tissue/min; CBF = 39.3 ± 7.8 cc/100 g/min; CBV = $3.2 \pm 0.7\%$; OER = $47.5 \pm 5.0\%$; $CMRO_2$ = 170.9 ± 31.6 μ mol/100 g/min.

ACKNOWLEDGMENTS

The authors thank the staff of the Brain Imaging Center for their dedicated work on this project, and Miss Carolyn Elliot for assisting in the preparation of this manuscript.

This study was supported by the Medical Research Council of Canada Program Grant SP-5, USPH Grant 1 ROI NS 22230-01A1, and the Killam Scholarship Fund and the Clive Baxter Research Fund of the Montreal Neurological Institute.

REFERENCES

1. Wilson CB. Current concepts in cancer. Brain tumors. *N Engl J Med* 1984; 300:1469-1471.
2. DiChiro G, Brooks RA, Patronas NJ, et al. Issues in the in vivo measurement of glucose metabolism of human central nervous system tumors. *Ann Neurol* 1984; 15:S138-S146.
3. Rhodes CG, Wise RJS, Gibbs JM, et al. In vivo disturbances of the oxidative metabolism of glucose in human cerebral gliomas. *Ann Neurol* 1983; 14:614-626.
4. Patronas NJ, DiChiro G, Kafta C, et al. Prediction of survival in glioma patients by means of positron emission tomography. *J Neurosurg* 1985; 62:816-822.
5. Karnofsky D, Burchenal JH. The clinical evaluation of chemotherapeutic agents in cancer. In: MacLeod CM ed. Evaluation of chemotherapeutic agents. New York: Columbia University Press, 1949: 191-205.
6. Cooke BE, Evans AC, Fanthome EO, et al. Performance figures and images from the Therascan-3128 positron emission tomograph. *IEEE Trans Nucl Sci* 1984; NS31:640-644.
7. Cooke BE, Evans AC. A phantom to assess quantitative recovery in positron tomographs. *J Comput Assist Tomogr* 1983; 7:876-880.
8. Strother SC, Thompson CJ, Evans AC. Testing quantitation in PET [Abstract]. *J Nucl Med* 1984; 25:P107.
9. Bergström M, Litton J, Erikson L, et al. Determination of object contour from projections for attenuation correction in cranial positron emission tomography. *J Comp Assist Tomogr* 1982; 6:365-372.
10. Diksic M, Jolly D. Remotely operated synthesis of 2-deoxy-2 18 F fluoro-D-glucose. *Int J Appl Radiat Isot* (in press)
11. Evans AC, Diksic M, Yamamoto YL, et al. A method for the simultaneous determination of regional rate constants for the uptake of 18 F labelled 2-fluoro-2-deoxy-D-glucose and regional blood volume. *J Cereb Blood Flow Metab*: in press
12. Phelps ME, Huang SC, Hoffman EJ, et al. Tomographic measurement of local cerebral glucose metabolic rate in humans with 18 F-L-fluoro-2-deoxy-D-glucose; validation of method. *Ann Neurol* 1979; 6:371-388.
13. Sokoloff L, Reivich M, Kennedy C, et al. The 14 C-deoxyglucose method for the measurement of local cerebral glucose utilization: theory, procedure, and normal values in the conscious and anesthetized albino rat. *J Neurochem* 1977; 28:897-916.
14. Brooks R. Alternative formula for glucose utilization using labelled deoxyglucose. *J Nucl Med* 1982; 23:538-539.
15. Huang SC, Phelps ME, Hoffman EJ, et al. Noninvasive determination of local cerebral metabolic rate of glucose in man. *Am J Physiol* 1980; 238:E69-E82.

16. Frackowiak R, Lenzi GL, Jones T, et al. Quantitative measurement of regional cerebral blood flow and oxygen metabolism in man using ^{15}O and positron emission tomography: theory, procedure and normal values. *J Comput Assist Tomogr* 1980; 4:727-736.
17. Lammertsma A, Jones T, Frackowiak R, et al. A theoretical study of the steady state model for measuring regional cerebral blood flow and oxygen utilization using oxygen-15. *J Comput Assist Tomogr* 1981; 5:544-550.
18. Kearfott KJ, Junck L, Rottenberg DA. ^{11}C -dimethylxoxazolidinedione (DMO): biodistribution, estimates of radiation absorbed doses, and potential for positron emission tomography (PET) measurement of regional brain tissue pH. *J Nucl Med* 1983; 24:805.
19. Rottenberg DA, Ginos JZ, Kearfott KJ, et al. In vivo measurement of brain tumor pH using ^{11}C -DMO and positron emission tomography. *Ann Neurol* 1985; 17:70.
20. Baron JC, Rougemont D, Soussaline F, et al. Local interrelationships of cerebral oxygen consumption and glucose utilization in normal subjects and in ischemic stroke patients: a positron tomography study. *J Cereb Blood Flow Metab* 1984; 4:140-149.
21. Nais AHW. Radiation biology. In: Thomas DGT, Graham DI, eds. Brain tumors. London: Butterworths, 1980:168-181.
22. Burger PC, Kamenar E, Schold C, et al. Encephalomyelopathy following high-dose BCNU therapy. *Cancer* 1981; 48:1318-1327.
23. Kapp J, Vance R, Parker JL, et al. Limitations of high-dose intra-arterial 1,3 bis (2-chloroethyl)-1-nitrosourea (BCNU) chemotherapy for malignant gliomas. *Neurosurg* 1982; 10:715-719.
24. Kato A, Diksic M, Yamamoto YL, et al. Regional cerebral blood flow and metabolism in human malignant gliomas studied by PET. *J Cereb Blood Flow Metab* 1985; 5:S49-S50.
25. Yamada K, Hayakawa T, Ushio Y, et al. Regional blood flow and capillary permeability in the ethylnitrosourea-induced rat glioma. *J Neurosurg* 1981; 55:922-928.
26. Hossmann KA, Niebuhr I, Tamura M. Local cerebral blood flow and glucose consumption of rats with experimental gliomas. *J Cereb Blood Flow Metab* 1982; 2:25-32.
27. Blasberg RG, Molnar P, Horowitz M, et al. Regional blood flow in RT-9 brain tumors. *J Neurosurg* 1983; 58:863-873.
28. Groothuis DR, Blasberg RG, Molnar P, et al. Regional blood flow in avian sarcoma virus (ASV)-induced brain tumors. *Neurology* 1983; 33:686-696.
29. Groothuis DR, Fischer IM, Pasternal J, et al. Regional measurements of blood flow in experimental RG-2 rat gliomas. *Cancer Res* 1983; 43:456-459.
30. Kato A, Sako K, Diksic M, et al. Regional glucose utilization and blood flow in experimental brain tumors studied by double tracer autoradiography. *J Neuro-Onc* 1985; 3:271-283.
31. Wise RJS, Thomas DGT, Lammertsma AA, et al. PET scanning of human brain tumors. *Prog Exp Tumor Res* 1984; 27:154-169.
32. Vaupel P. Oxygen supply to malignant tumors. In: Tumor blood circulation. Cleveland: CRC Press, 1979.
33. Herscovitch P, Raichle M. Effect of tissue heterogeneity on the measurement of cerebral blood flow with the equilibrium C^{15}O_2 inhalation technique. *J Cereb Blood Flow Metab* 1983; 3:407-415.
34. Lammertsma AA, Jones T. Correction for the presence of intravascular oxygen-15 in the steady-state technique for measuring regional oxygen extraction ratio in the brain: 2. Results in normal subjects and brain tumor and stroke patients. *J Cereb Blood Flow Metab* 1983; 3:425-431.
35. Lammertsma AA, Wise RSJ, Gibbs J, et al. The pathophysiology of human cerebral tumors and surrounding white matter and remote cortex. *J Cereb Blood Flow Metab* 1983; 3:S9-S10.
36. Kendall B. Neuroradiology. In: Thomas DGT, Graham DI, eds. Brain tumors. London: Butterworths, 1980:231-267.
37. Ito M, Lammertsma AA, Wise RSJ, et al. Measurement of regional cerebral blood flow and oxygen utilization in patients with cerebral tumors using ^{15}O and positron emission tomography: analytical techniques and preliminary results. *Neuroradiology* 1982; 23:63-74.
38. DiChiro G, Brooks RA, Sokoloff L, et al. Glycolytic rate and histologic grade of human cerebral gliomas: a study with ^{18}F fluorodeoxyglucose and positron emission tomography. In: Phelps ME, Heiss W-D, eds. Positron emission tomography of the brain. Berlin: Springer-Verlag, 1983:181-191.
39. Warburg O. The metabolism of tumors. London: Arnold Constable, 1930:75-327.
40. Dickens F, Simer F. The metabolism of the normal and tumor tissue. *Biochem J* 1930; 24:1301-1326.
41. MacBeth RAL, Bekesi JG. Oxygen consumption and anaerobic glycolysis of human malignant and normal tissue. *Cancer Res* 1962; 22:244-248.
42. DiChiro G, DeLa Paz RL, Brooks RA, et al. Glucose utilization of cerebral gliomas measured by ^{18}F fluorodeoxyglucose and positron emission tomography. *Neurology* 1982; 32:1323-1329.
43. Kessler RM, Ellis JR, Eden M. Analysis of emission tomographic scan data: limitations imposed by resolution and background. *J Comput Assist Tomogr* 1984; 8:514-522.
44. Weber MJ, Salter DW, McNair TE. Increased glucose transport in malignant cells: analysis of its molecular basis. In: Arnott MS, van Eys J, Wang Y-M, eds. Molecular interrelations of nutrition and cancer. New York: Raven Press, 1982:183-189.
45. Molnar P, Blasberg RG, Horowitz M, et al. Regional blood-to-tissue transport in RT-9 brain tumors. *J Neurosurg* 1983; 58:874-884.
46. Molnar P, Blasberg RG, Groothuis D, et al. Regional blood-to-tissue transport in avian sarcoma virus (ASV)-induced brain tumors. *Neurology* 1983; 33:702-711.
47. Paxton HD. Quantitative biochemistry of brain tumors and analogous normal tissue. *Neurology* 1959; 9:367-370.
48. Timperley WR. Glycolysis in neuroectodermal tumors. In: Thomas DGT, Graham DI, eds. Brain tumors. London: Butterworths, 1980:145-167.
49. DeLa Paz RL, Patronas NJ, Brooks RA. Positron emission tomography of gray matter glucose utilization by brain tumors. *AJNR* 1983; 4:826-829.
50. Brock M, Hadjidimos A, Deruaz JP, et al. Regional cerebral blood flow and vascular reactivity in cases of brain tumor. In: Ross Russel RW, ed. Brain and blood flow. London: Pitman, 1971:281-284.
51. Reulen HJ, Medzihradsky F, Enzenbach R, et al.

- Electrolytes, fluids, and energy metabolism in human cerebral edema. *Arch Neurol* 1969; 21:517-525.
52. Arnold JB, Junck L, Rottenberg DA. In vivo measurement of regional brain and tumor pH using ^{14}C dimethyloxazolidinedione and quantitative autoradiography. *J Cereb Blood Flow Metab* 1985; 5:369-375.
53. Brooks DJ, Beaney RP, Thomas DGT, et al. Studies on regional cerebral pH in patients with cerebral tumors using continuous inhalation of $^{11}\text{CO}_2$ and positron emission tomography. *J Cereb Blood Flow Metab* 1986; 6:529-535.
54. Rapoport SI. Blood-brain barrier in physiology and medicine. New York: Raven Press, 1976: 129-138.